Flat Fading Channel – Modelling via HMM and HSMM

[1]Dr. S. Durairaj, [2]G. Rema

[1]Associate Professor, Kamaraj College, Thoothukudi, India.
[2]Assistant Professor, Lekshmipuram College, Neyoor, India.

***Abstract*-Fading phenomena impact the performance of wireless communication systems. We proposed Modified Hidden Semi-Markov Model (MHSMM) for modeling the flat fading envelope process. The properties of the envelope process are dominated by the physical fading processes and speeds of the mobile terminal. Thus, the statistics of the fading process may be non-stationary, due to different fading conditions over some time durations. The MHSMM incorporate these time-variant statistics of the envelope process in a single model, which facilitates computations of the envelope probability density function and the auto correlation function. The study provides estimation schemes by simulation. It verifies the advantages of MHSMM and also the effectiveness of the associated parameter estimation schemes.**

***Keywords*-Signal Fading, HMM, HSMM, Modelling**

I. INTRODUCTION

Modeling of the fading in the communication channels is of interest for a long time. A common feature in these models is that all of them have memory. Gaussian process modeling, though attempted is difficult in this type of systems. HMM has a unique feature of helping in the evaluation of various probabilistic features through the EM algorithms. One more important factor is the simplicity of the model for which HMM is more appropriate and hence this attempt.

II. FADING CHANNEL MODEL

Lab x(t) be low pass equivalent of the communicatedsignal with the inphase component$x_I(t)$ = Re{x(t)} and quadrature compound $x_Q(t)$=Im{x(t)}. Consider a frequency non selective channel with additive noise n(t). This channel is modelled as: [J.G.Proakis [15]].

$$y(t) = c(t)\, x(t) + n(t) \quad (1)$$

Where,y(t) is the acknowledged signal and the fading is modelled by the complex random process c(t). Different models are there which are based on different assumptions on c(t) and n(t).

Normally it is assumed that n(t) is zeromean complex AWGN(additive white Gaussian noise) and c(t) is complex stationary zero-mean Gaussian process with identical and independently distributed (i.i.d) real and imaginary parts. The p.d.f. of a sequence C_K=($c(t_1)$, $c(t_2)$, …, $c(t_k)$) has the form.

$$f(C_K)=(2\pi)^{-K}\,|D|\,\exp(-0.5\,\mathrm{Re}\{C_K\, D\, C_K^H\}) \quad (2)$$

Where |D| denotes the determinant of D, C_K^H denotes the conjugate transpose of C_K, and D^{-1} is the process variance co-variance matrix

$$D^{-1} = [R(t_j - t_i)]_{K,K} \quad (3)$$

Where R(t) is the auto correlation function of the process. The multi- dimensional distribution has a related form.

This model is called a Rayligh fading since its envelope $\alpha(t) = |C(t)|$ is Rayligh distributed

$$P_r\{\alpha(t) < \alpha\} = 1 - \exp(-0.5\, a^2 |\, \mu)$$

Different fading models are based on the different basic conventionsnearly the power spectral density S(f) or, equivalently, the auto correlation function R(τ) of c(t):

Here we use

$$S(f) = \mu/\pi\sqrt{f_D^2 - f^2},\ R(\tau) = \mu\, J_0(2\pi\, f_D\, |\, \tau\, |) \quad (4)$$

Here $J_0(.)$ is the Bessel function of the first kind, f_D is the maximal Doppler frequency, and μ is the power of the fading process c(t). We call this model as the clarke's model [6]. It is known that stationary Gaussian stochastic process can be modelled by filtering white Gassian noise ω(t) [15]

On the other hand, it could be simulated by the next equation

$$C(t) = 2\sum_{i=1}^{N} e^{j(i\pi|N+1)}\,\mathrm{Cos}\,(2\pi f_D t\,\mathrm{Cos}\,\frac{2\pi i}{4N+2}) + \sqrt{2}\,\cos 2\pi\, f_D t \quad (5)$$

In applied systems, the communicated signal x(t) has the form

$$x(t) = \sum_k x_k\, P(t - k_\Delta) \quad (6)$$

Where $1/\Delta$ is the symbol rate, x_K is the transmitted symbol value, a complex number, matching to a point of the signal collection, and p(t) represents the shaping pulse. If we assume that C(t) is slowly varying s_o that it is closely constant above a symbol duration Δ, the sampled output of the coherent demodulator trailed by the receiver matched filter which can be estimated by

$$Y_k = c_k x_k + n_k \quad (7)$$

Where n_k is the sample of the filtered Gaussian noise and $c_k = c(k\Delta)$ is a sample of the fading process.

III. FADING ENVELOPE MODEL

For relaxed slow fading, the performance of communication system depends mainly on the value of the envelope $\alpha(t) = |c(t)|$. The envelope could be defined by its multidimensional p.d.f. which we can derive from (2). That is

$f(\alpha_k)=(2\pi)^{-k} |D| \alpha_1 \alpha_2 \dots \alpha_k \int_0^{2\pi}$ (k) …

$\int_0^{2\pi}$ $\exp(-0.5\, \alpha_k G\, \alpha_k^T) d\theta_1 \dots d\theta_k$ (8)

Here $\alpha_i = \alpha(t_i)$, $\theta_i = \theta(t_i)$, G is the matrix whose i, j_{th} element is

$g_{ij} = d_{ij} \cos(\theta_i - \theta_j)$, where d_{ij} is the element in the i_{th} row and j^{th} column of D, and $\alpha_k=(\alpha_1 \alpha_2 \dots \alpha_k)$

If k=1, we have the Rayleigh p.d.f.

$f(\alpha_1) = \alpha_1 \mu^{-1} \exp(-0.5\, \alpha_1^2/\mu)$,

$\mu = R(0) = \sigma^2$ (9)

If k=2, we have, the Joint p.d.f

Since the correlation function $R(\tau)$ tends to zero and c_k is Gaussian it can be approximated with a Markov process if m is large enough so that $R(m\,\Delta) \approx 0$ (since c_k and c_{k+m} become uncorrelated and hence independent). The envelope transitional PDF has the form

$a(\alpha_K | \alpha_{k-m}^{k-1}) = f(z_t / z_{t-m}^{t-1})$

Since the correlation function $R(\tau)$ tends to zero and c_k is Gaussian it can be approximated with a Markov process if m is large enough so that $R(m\,\Delta) \approx 0$ (because c_k and c_{k+m} become uncorrelated and hence independent). The envelope transitional p.d.f has the form

$a(\alpha_k | \alpha_{k-m}^{k-1}) = f(\alpha_{k-m}^{k}) / f(\alpha_{k-m}^{k-1})$ (11)

where $\alpha_{k-m}^{k-1} = (\alpha_{k-m}, \alpha_{k-m+1}, \dots \alpha_{k-1})$. Thememory size m of the process could be strongminded using an estimate accuracy measure (an example is given in section (ii). For the simple Markov Process (m=1) the transition p.d.f is the Ricianp.d.f.

If we perform the envelope quantization into N levels, the quantized process $\{\rho_k\}$ can be approximated by the Markov Chain with N states. In particular, for the simple Markov Chain (m=1) we have the transition probabilities.

$a_{ij} = \int_{q_{L,i}}^{q_{H,i}} \int_{q_{t,i}}^{q_{H,j}} f(\alpha_1, \alpha_2)\, d\alpha_1,$

$d\alpha_2 / \int_{q_{L,i}}^{q_{H,j}} f(\alpha)\, d(\alpha)$ (12)

where $f(\alpha_1, \alpha_2)$ is given by (10). If the quantization intervals are small, we can write $a_{ij} = a(\rho_j|\rho_i)\,(q_{H,j} - q_{L,j})$, for j = 1…N and $a_{iN} = 1 - \sum_{i=1}^{N-1} a_{ij}$. The first-order approximationmodel is satisfactory for fading of Rayligh whose density of power spectral is given by (4). This estimate, moreover, is reasonable for comparatively short intervals only.

To approximate the Bessel function coming out of (4) we need Markov Chains with large memory. Since the number of states grows exponentially with the process memory, this approach is not practical.

(ii) Quantized Autoregressive and Moving Average (ARMA) using the standard methods of the infinite impulse response (IIR) filter design [7] we can

$f(\alpha_1\, \alpha_2) = \frac{\alpha_1 \alpha_2}{\mu^2(1-\lambda^2)} \exp$

$[\, - \frac{\alpha_1^2 + \alpha_2^2}{2\mu(1-\lambda^2)}] \cdot I_0 (\frac{\alpha_1 \alpha_2}{\mu} \frac{\lambda}{1-\lambda^2})$ (10)

Where $\lambda = R(t_2-t_1) / R(0)$, $I_0(.)$ is the modified Bessel function of the first kind.

The above model is difficult to use in applications in which distribution of high-dimension k is needed. In such cases, the Monte Carlo method can be applied, but the HMM is simpler to apply.

IV. MARKOV MODELS

(i) Multiple Markov chains

Multiple Markov processes z_1^∞ are processes with finite memory. If the process has memory m, the conditional p.d.f. of z_t given all the past observations z_1^{t-1}, depends only on the m previous observations z_{t-m}^{t-1} (where z_i^j denote $z_i, z_{i+1}, .. z_j$), ie.

$f(z_t | z_1^{t-1}) = f(z_t / z_{t-m}^{t-1})$

approximate the fading power spectral density with the function.

$S(f) = \frac{|\sum_{i=0}^{P} d_i z_i^2|^2}{|1+\sum_{i=1}^{P} h_i z_i|^2}$, $d_0 \neq 0$ (13)

Here $z = e^{-2\pi i f}$. In the case c(t) can be modelled by the complex ARMA process

$C_k = \sum_{i=1}^{P} h_i c_{k-i} + v_k$, $v_k = \sum_{i=0}^{q} d_i n_{k-i}$ (14)

wheren_i, are i.i.d. Gaussian variable. If q = 0 we have a AR process (v_k=do n_k). The ARMA process of approximation of fading is a special case of a Markov process whole state is defined by the vector $c_{k-p}^{k-1} = (c_{k-p}, c_{k-p+1}, \dots, c_{k-1})$,

$n_{k-q}^{k-1}=(n_{k-q}, n_{k-q+1}, \dots, n_{k-1})$. For obtaining the Markov chain with the finite number of states, we need to quantize these vectors. This approach is more directly related to approximating the auto-correlation function than the one considered in this previous section. Apart from this, it allows us to use the standard methods of filter design for building the model. In Butter worth filter [2,14] we have a simple markov process. The fading envelope $\alpha_k = |c_k|$ is a function of the Markov Chain and, hence, it is a special case of an HMM. The ARMA model complexity grows linearly with process memory. This model is difficult to use for calculating model statistics. As in the case of the multiple Markov chains, the size of this model transition probability matrix grows exponentially with the process memory. The matrix is large, but sparse.

(iii) Birth-Death Process

Birth and Death processes are a special case of a Markov model [17, 22]. These models assume that the quantized fading amplitude from the current i^{th} level can jump only to the adjacent levels, ie. $a_{ij}=0$ if $|i-j|>1$. If a_{ii} is large, this model allows us to model a slowly varying processes.

It is possible to improve this model by splitting each state i into t_w i_s and i_e, depending on thetransition slope [17]. Here i_s corresponds to the start of fading below the level q_i and i_e corresponds to its end.

The accuracy of this model depends on the selection of quantization levels. The quantization levels must satisfy two conditions: a_{ij} given by (12) should be close to zero for |j-1|>1 and the original model state duration distributions should be close to the exponential distributions. It is difficult to satisfy these two conditions. In order to fit the exponential state duration the number of quantization levels must be large, but in this case the probabilities a_{ij} of transitions to the nonadjacent levels (|i-j|>1) are not negligibly small. The model approximation can be improved by allowing nonadjacent level jumps.

(iv) **Monte Carlo method**

Since it is difficult to evaluate the integrates which are needed for the Markov Process approximation, the model parameters can be estimated using computer simulation. After sampling and quantizing the envelope $\alpha(t)=|c(t)|$ we obtain the sequence ρ_1^T. Now we can apply the methods of fitting Markov Chains to experimental data as given in [6]. The state transition probabilities are estimated by

$$\hat{a}_{ij} = n_{ij} \mid n_i,\ n_i = \sum_{j=1}^{n} n_{ij} \qquad (15)$$

Where n_{ij} is the number of transitions from state i to state j.

V. Modeling of Fading by HMM

A HMM is a probabilistic function of a Markov Chain and can be defined as {S, X, π, A, B(x)} where $S=\{s_1, s_2,\ldots, s_n\}$ is the set of states of the

A. Autocorrelation Function of HMM

To compute the auto correlation function

$R(\tau) = E(x_k, x_{k+\tau})$

We evaluate the probability densities $p(x_1^t)$ of a HMM output sequences $x_1^k = (x_1, x_2, \ldots, x_k)$. These probability densities have the form [21].

$$p(x_1^k) = \pi\ P(x_1)\ P(x_2)\ \ldots\ P(x_k)\ 1 = \pi \prod_{i=1}^{k} P(x_k) 1 \qquad (20)$$

where P(x) = AB (x) is the matrix of p.d.f of x and 1 is the column matrix of ones

Using these equations, we can write

$R(O) = \pi E(x^2)1$, $R(\tau) = \pi E(x)\ A^{\tau-1}\ E(x)1$,

$R(-\tau) = R\ \tau$, for $\tau>0$

Where

$$E(x) = \int_{-\infty}^{\infty} x\ P(x)dx,\quad E(x^2) = \int_{-\alpha}^{\alpha} x^2 P(x)dx$$

are the matrix expectations of x and x^2, respectively.

It follows from these equations that the z-transformation of R(τ) for τ>0 is a rational function.

$$R(z)=\sum_{\tau=1}^{\infty} R(\tau)\ z^{-\tau} = \pi\ E(x)\ (I_z-A)^{-1}\ E(x)1 \qquad (21)$$

Expanding it into partial fractions we obtain

$$R(z) = \sum_{j=1}^{r} \sum_{i=1}^{m_j} D_{ij}\ (z-\lambda_j)^{-i} \qquad (22)$$

Where λ_j are the eigen values of the matrix A. Thus

$$R(\tau) = \sum_{j=1}^{r} \sum_{i=1}^{m_j} D_{ij}\ \binom{\tau-1}{i-1}\lambda_j^{\tau-i},\ \tau > 0 \qquad (23)$$

In particular, if all the eigen values are different, R(τ) is a mixture of exponential functions.

$$R(\tau) = \sum_{j=1}^{r} D_{1j}\lambda_j^{\tau-1},\ \tau > 0 \qquad (24)$$

Markov chain, X is the HMM output (observation) set, π is a vector of state initial probabilities, $A=[a_{i,j}]_{n,n}$ is a matrix of state transition probabilities $a_{ij}=Pr\{S_j \mid S_i\}$, and $B(x)=diag\ \{b_j\ (x)\}$ is a diagonal matrix of the output $x \in X$ conditional probability densities in state s_j. If X is discrete, B(x) is a matrix of probabilities $b_i(x)=Pr\{x|s_j\}$ we denote the states by their indexes ($s_i=i$).

Alternatively, HMM can be represented by the so-called state space equations.

$$U_{k+1} = G(u_k, \xi_k) \qquad (16)$$

$$x_k = H(u_k, \eta_k) \qquad (17)$$

when ξ_k and η_k are i.i.d variable. Indeed, it follows from (16) that $\{u_k\}$ is a Markov Process, generally with an infinite number of states. If G(u, v) has a finite discrete range, however, then we have a Markov Chain with the finite number of states and state-transition probabilities.

$$a_{ij}=Pr\{u_{k+1} = j \mid u_k= i\}= Pr\{G(i, \xi) = j\} \qquad (18)$$

According to (17), observations x_K are conditionally independent variable, given the state sequence, and have the following p.d.f.:

$$F_i(x) = Pr\{x_k<x|u_k=i) = Pr\{H(i, \eta) < x\} \qquad (19)$$

Conversely, for any HMM we can find G(i, ξ) and H(i, η) by inverting (18) and (19), respectively,

To know the limitations of HMM approximations, we need to know about the auto correlation function of HMM's.

If follows from these equations that a HMM power spectral density is a rational function for $z = e^{2\pi jf}$

$$S(f) = \pi E(x^2) - [\pi E(x)1]^2 + \pi\ E(x)\ [I-Qz)^{-1} + (I-Q\bar{z}^{1})^{-1}]E(x)\ 1$$

where

$Q^{\tau-1} = A^{\tau-1} - 1\ \pi$

According to (23), the autocorrelation function must have the form

$$R(\tau) = \sum_{j=1}^{r} [P_j(\tau)\ Cos\ \gamma_j\tau + Q_j(\tau)\ sin\ \gamma_j\ \tau]\ q_j^{\tau},\ \tau > 0$$

where $P_j(\tau)$ and $Q_j(\tau)$ are polynomials $q_j = |\lambda_j|$ and $\gamma_j = arg(\lambda_j)$. If all eigenvalues are different R(τ) takes the form:

$$R(\tau) = \sum_{j=1}^{\tau} P_j q_j^{|\tau|}\ ,\ Cos\ \gamma_j\tau.$$

This class of functions are rich enough to approximate any autocorrelation function. Let us now have different methods of approximating the fading process with HMM's.

VI. Parameter estimation for HMM

Once a class of models are selected, we have to fit a model from this class to the fading process. There are several methods of fitting the model.

A. Parameter estimation by the method of moments

The method of moments consists of equating the moments of the two models and solving the corresponding equation. For easily solving one of the models is represented by its experimental data. For example an approximation by Rayleigh fading by a HMM [17]

There are several problems with the method of moments one of the problems is that the system of equations for the moments is often ill posed. The The other problem is that the moment selection is quite arbitrary. For example, we can find a HMM whose autocorrelation function is close to that of the fading process. However, this does not mean that the multidimensional probabilities associated with these processes are close.

Hence, the method of moments could be used for selecting initial values of the model parameters which are then improved by more sophisticated statistical algorithms.

B. Approximating Multidimensional probability Densities

One of the most powerful methods of approximating a stochastic process with a HMM consists of fitting multidimensional probability distributions of a HMM to that of the original process. The HMM parameters can be obtained as those which minimize the Kullback-Lecbler divergence

$$\theta = \arg\min K(f \parallel p_\theta) \qquad (25)$$

where $K(f \parallel p_\theta) = \int_{X^k} f(x_1^k) \log\frac{f(x_1^k)}{p(x_1^k)} d\, x_1^k$ (26)

f(.) and p_θ(.) are given by (8) and (20), respectively and θ is the HMM parameter vector. The minimum in (25) can be obtained iteratively by the EM algorithm [21]: its version for fitting HMM's is called the Baum-Welch algorithm [1]. The computational efficiency of the algorithm depends on the nature of the statistical data. For slowfading, a HMM approximation should be close to the birth-and-death process. Since the model matrix is sparse, direct application of the previous equations for the slow fading data is very efficient we can improve the algorithm efficiency by using the matrix fast exponentiation [21]. Another improvement can be achieved by taking advantage of the following property of the Baum-welch algorithm if $a_{ij,p}$= 0 at some iteration step p, their $a_{ij,p+1}$=0. Hence, at each interation we can replace small elements with zeroes and apply the sparse matrix multiplication algorithms.

Alternatively, we can start with the birth-and-death process approximation. If the state transitions satisfy the markovian property, but the state duration distributions are not exponential, we have a semi-markov process approximation which can be transformed into a HMM as given below [19].

In the above, the diagonal matrices A_i represent the transitions between states of the HMM that correspond to the i^{th} quantization level of the fading process, ie the probability of observing the level in those states is equal to one.

The matrix geometric distribution parameters can be estimated using the Baum-Welch algorithm if we notice that the state holding process is a binary HMM where state transition probability matrix is E_i.

To illustrate this method, we use simulation. The fading process is simulated using the moments are the same for quite different models. The model structure is usually selected using our intution and the model accuracy must be evaluated separately.

$$\begin{pmatrix} 0 & \bar{a}_{12} & \dots & \dots & \bar{a}_{1m} \\ \bar{a}_2 & 0 & \dots & \dots & \bar{a}_{2m} \\ \dots & \dots & \dots & \dots & \dots \\ \dots & \dots & \dots & \dots & \dots \\ \bar{a}_{m1} & \bar{a}_{m2} & \dots & \dots & 0 \end{pmatrix} \qquad (27)$$

Let be the transition process transition probability matrix. Suppose that we are able approximate the state duration distributions with the phase-type matrix-geometric distribution.

$$p_i(x) = \mu_i A_i^{x-1} b_i \qquad (28)$$

Where A_i is a square matrix, μ_i, is a row vector, and b_i is a column vector such that

$$E=\begin{pmatrix} A_i & b_i \\ \mu_i & 0 \end{pmatrix}$$

is a stochastic matrix, that is all its elements are non-negative and each row sums to one $E_i1=1$. Then the semi-Markov process is equivalent to a HMM whose state transition probability matrix is given by

$$A = \begin{pmatrix} A_1 & \bar{a}_{12} b_1 \mu_2 & \dots & \dots & \bar{a}_{1m} b_1 \mu_m \\ \bar{a}_{21} b_2 \mu_1 & A_2 & \dots & \dots & \bar{a}_{2m} b_2 \mu_m \\ \dots & \dots & \dots & \dots & \dots \\ \dots & \dots & \dots & \dots & \dots \\ \bar{a}_{m1} b_m \mu_1 & \bar{a}_{m2} b_m \mu_2 & & & A_m \end{pmatrix}$$

Rician process, with its acf as described in clarke [3]. The Rician marginal envelope distribution is taken as

$$f_{Rice}(x) = \frac{2(k_R+1)x}{\Omega} \exp\left(-k - \frac{(k_R+1)x^2}{\Omega}\right) \times I_o \left(2x\sqrt{\frac{k_R(k_R+1)}{\Omega}}\right), \qquad (30)$$

where $x \geq 0$, $k_R \geq 0$, $\Omega \geq 0$. For a transmitter with the carrier frequency f_c, the mobility speed v, and the speed of the electromagnetic wave c, the maximum Doppler frequency shift f_D in the clarke model is expressed as f_D=vfc/c. The envelope process is simulated to be piece-wise stationary, with different

sets of parameters in the Rician process and the clarkeacf at different states. The lognormal distribution is used to model the state duration pdf as

$$f_{\text{lognormal}}(t; \mu_{ln}, \sigma) = \frac{\exp[-(ln(t)-\mu_{ln})^2/(2\sigma^2)]}{t\sigma\sqrt{2\pi}}, \quad (31)$$

where $0 \le t < \infty \le \mu_{ln} \le \infty$, $\sigma \ge 0$

In the GSM system [8], the normal frequency is 900 MHz. The power level can be from 39 dbm to 5dbm. Thus, a 10 db difference between the LOS and the NLOS assumption is apt and reasonable. There are four states in the simulation, described as follows.

State: 1 The mobile is assumed to be moving in a high speed at 30 mls, in the NLOS scenario. The mean of the received signal envelope is -10 db, with respect to the reference level. Based on the 900 MHz of the GSM carrier frequency, the Doppler shift is f_D=90 Hz. Since it is in the NLOS scenario, a reasonable value of K_R in the Rician process is taken to be 1, ie. no dominant components in the scattered signals. The

The Doppler shift is f_D=9 H_z. Due to the NLOS scenario, the K_R in the Rician process is taken to be 1. The state duration is generated by the lognormal distribution with a mean of 50 seconds, with parameters of $(\mu_{ln}, \sigma) = (3, 0.8958)$ in (31).

STEP : 4 The mobile, here is, assumed to be moving in a low speed at 3 m/s, in the LOS scenario. The mean of the received signal envelope is 0db. The Doppler shift is f_D=9 Hz. In view of the LOS scenario, the K_R in the Rician process is taken to be 10. The state duration is generated by the lognormal distribution with a mean of 70 seconds, with parameter values $(\mu_{ln}, \sigma) = (3.5, 0.6146)$ in (31).

The state transition probability is taken as

$$P = \begin{pmatrix} 0 & 0.21 & 0.21 & 0.62 \\ 0.32 & 0 & 0.52 & 0.21 \\ 0.32 & 0.32 & 0 & 0.41 \\ 0.41 & 0.41 & 0.21 & 0 \end{pmatrix}$$

Which specifies the steady state probability to be π = [0.2528 0.2336 0.2252 0.2884]. In our simulation, the envelope process is generated by the above parameters inside state 1 to 4, with state transitions governed by P. The initial state is generated by π. The envelope process is simulated for 10398 seconds, where 400 states are realized. The envelope process is sampled at 1000 samples/second. After obtaining the envelope sequence, we estimated the MHSMM (Modified Hidden Semi-Markov Model) parameters by the sequence segmentation step given below.

C. MHSMM Definition and notations:

byth MHSMM, those $\{x_1, x_2, \ldots, x_n\}$ can be seen as the rvs representing the observable outputs of the

state duration is generated by the lognormal distribution with 10 second as mean, and the parameters $(\mu_{ln}, \sigma) = (2, 0.7779)$ in (31).

State : 2 The mobile is assumed to be moving in a high speed at 30m/s in the LOS scenerio. The mean of the received signal envelope is odb, ie., equal to the reference level. The Doppler shift is f_D = 90Hz. Because of the LOS scenario, the K_R in the Rician process is taken to be 10, ie., the dominant component has the envelope 10 times larger than the envelopes of the scattered signals. The state duration is generated by the lognormal distribution with a mean equal to 30 seconds, with parameters of (μ_{ln}, σ)=(2.5, 0.9954) in (31).

State 3: The mobile is assumed to be moving in a low speed at 3 m/s, in the NLOS scenario. The mean of the received signal envelope is -10 db.

The MHSMM consists of many states with an individual stationery process representing each state. Embedded inside each state is a random process with its own statistics. Transitions among the states are specified by the transition probability matrix (tpm). An example of a four-state MHSMM is illustrated in Fig.1. The notations are explained as follows:

i. The number of states is denoted by M. The M states of the MHSMM are denoted by $\{S_1, S_2, \ldots, S_M\}$. The time duration from the starting of one state to the end of the state is defined as one epoch. The state in the i^{th} epoch is defined as q_i. The duration of the i^{th} epoch is denoted as τ_i.
ii. The MxMtpm is denoted by A. The elements in A are denoted as a_{ij}, where $a_{ij} = P(q_{I+1} = S_j / q_I = S_i)$ for any i, j, $1 \le i, j \le M$, and I is the index of any valid epochs. Since the state duration is explicitly specified in the MHSMM, without any loss of generality, we assume that the state self-transition probability to be zero, iea$_{ii}$=0 for any i, $1 \le i \le n$.
iii. The 1xM steady state probability vector of the $\{S_1, S_2, \ldots, S_M\}$ states is denoted by $\pi = [\pi_1 S_1, \pi_2 S_2, \ldots, \pi_M S_M]$, where π_i is the steady – state probability of S_i for any valid i.
iv. The state duration pdfs corresponding to $\{S_1, S_2, \ldots, S_M\}$ are individually denoted by $\{P_{dur,s_{1(t)}}, P_{dur,s_{2(t)}}, \ldots, P_{dur,s_{m(t)}}\}$, for any i, $1 \le i \le M$, the $P_{dur,s_i(t)}$ can be interpreted as the p.d.f of an epoch length conditional on the state S_i.
v. The acfs corresponding to the states of $\{S_1, S_2, \ldots, S_M\}$ are individually denoted by $\{R_{s_1}(t), R_{s_2}(t), \ldots, R_{s_M}(t)\}$ are denoted by $\{P_{s_1}(x), P_{s_2}(x), \ldots, P_{s_M}(x)\}$individually. For the purpose of modeling the channel gains represented

MHSMM. The realization of the rvs are denoted by $\{x_1, x_2, \ldots, x_M\}$.

Based on the above notations, the following quantities can be derived.

1. For any valied state, steady – state percentage of time in the state S_i is given by

$$\frac{\pi_{S_i}\mu_{dur}(S_i)}{\Sigma\pi_{S_i}\mu_{dur}(S_i)} \qquad (6.1)$$

2. The overall envelope marginal p.d.f. can be computed by

$$P_x(x) = \frac{\pi_{S_1}\mu_{dur}(S_1)}{\Sigma\pi_{S_i}\mu_{dur}(S_i)} P_{s_1}(x) + \frac{\pi_{S_2}\mu_{dur}(S_2)}{\Sigma\pi_{S_i}\mu_{dur}(S_i)} P_{s_2}(x) + \cdots\cdots + \frac{\pi_{S_M}\mu_{dur}(S_M)}{\Sigma\pi_{S_i}\mu_{dur}(S_i)} P_{s_M}(x) + \ldots \qquad (6.2)$$

In the example of Fig.1, the state transitions are governed by the state transition probability a_{ij} for any i, j, $1 \le i, j \le 4$. Inside each state, the state duration pdf $P_{dur,s_i}(.)$ governs the state duration. The conditional envelope pdf $P_{s_i}(.)$ and the asf $R_{s_1}(.)$ govern the outputs of that state.

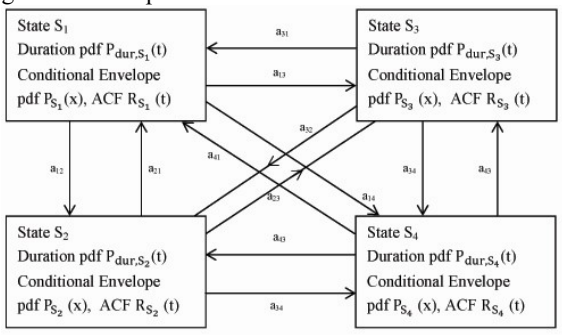

Fig.1 A-4 state example of MHSMM

D. Parameter Estimation of MHSMM

While applying the above model in practical situations, we need the estimates of the parameters of the MHSMM from a given of channel realizations. The proposed scheme includes two steps: the sequence segmentation step and the state parameter estimationstep. In the sequence segmentation step, we separate the observed channel sequence into segments corresponding to individual states of the MHSMM. Since these segments which are represented by the state process of the MHSMM must be approximately stationary within the individual states, the statistics are approximately equal within individual segments. On the other hand if the statistics are different between the segments represented by different states, then the sequence segment step has to be designed to detect segment boundaries by exploiting the changes of the statistics, e.g., the mean and the acf of the sequences. After obtaining the segments, we characterize each segment by its mean value and entropy value of the spectrum. We perform clustering algorithms to classify feature representations of the segments into clusters. Each segment of those clusters individually corresponds to a state of the MHSMM. In the state parameter estimation step, we use these segments, obtained from the sequence segmentation step, to estimate the state parameters of the states of the MHSMM.

E. Sequence Segmentation Steps

Here, we separate the observed channel sequence into segments corresponding to individual states of the MHSMM, by detecting the change of mean and acf values. The segments are then clustered to form states of the MHSMM. The cluster algorithm is based on similarities in the pairs of the mean and the acf values of the segments. By denoting the observed realizations of $\{X_1, X_2, \ldots, X_n\}$ as $\{x_1, x_2, \ldots, x_n\}$, the sequence segmentation step can be described as given below:

i. Compute the means of the observed channel gains based on a sliding window. This operation generates local means, $\{\mu_{t_1}, \mu_{t_2}, \ldots, , \mu_{t_n}\}$, corresponding to the time instants $\{t_1, t_2, \ldots, t_n\}$.

ii. Compute the spectrogram of the observed channel gains. This step generates the local spectra $\{X_{t_1}(f), X_{t_2}(f), \ldots, X_{t_n}(f)\}$, corresponding to the time instants $\{t_1, t_2, \ldots, t_n\}$. We use these local spectra to detect changes in the acts. Thus, the entropies of the local spectra serve as good indicators for changes in the acf's.

iii. Segment the local means $\{\mu_{t_1}, \mu_{t_2}, \ldots, , , \mu_{t_n}\}$ by using the sliding window segmentation approach [14]. We have to determine the timedetermined by segmenting $\{\mu_{t_1}, \mu_{t_2}, \ldots, , , \mu_{t_n}\}$, which are denoted as $\{T_{\mu,1}, T_{\mu,2}, \ldots, T_{\mu,k_\mu}\}$.

iv. Compute the sequence of the local entropies by computing the entropies of the absolute value of the local spectra, i.e,; the entropies of the energy distributions of:$\{|X_{t_1}(f)|, |X_{t_2}(f)|, |X_{t_3}(f)|, \ldots. |X_{t_n}(f)|\}$. The sequence of the entropies are denoted by $\{e_{t_1}, e_{t_2}, \ldots, e_{t_n}\}$.

v. Segment the $\{e_{t_1}, e_{t_2}, \ldots, e_{t_n}\}$ by the sliding window segmentation approach [14]. The purpose of this operation is to determine the time instants at which the $\{e_{t_1}, e_{t_2}, \ldots, e_{t_n}\}$ show changes. Each segment represents a process with its own approximately time-invariant entropy. That is, the segment boundaries $\{e_{t_1}, e_{t_2}, \ldots, e_{t_n}\}$ separate $\{x_1, x_2, \ldots, x_n\}$ into segments with approximately stationary entropies within the individual segments. The time instants of the segment boundaries, determined by segmenting $\{e_{t_1}, e_{t_2}, \ldots, e_{t_n}\}$, are denoted as $\{T_{e,1}, T_{e,2}, \ldots, T_{e,k_e}\}$.

vi. Obtain the candidates of the overall segment boundaries by sorting the union of the $\{T_{\mu,1}, T_{\mu,2}, \ldots, T_{\mu,k_\mu}\}$ and $\{T_{e,1}, T_{e,2}, \ldots, T_{e,k_e}\}$. In otherwords the obtained candidates of the segment boundaries $\{T_1, T_2, \ldots, T_{\mu,k_\mu}\}$ and

$\{T_{e,1}, T_{e,2}, \ldots, T_{e,k_e}\}$. }. In otherwords the obtained candidates of the segment boundaries $\{T_1, T_2, \ldots, T_{(k_\mu+k_e)}\}$ are equivalent to the instants where the $\{\mu_{t_1}, \mu_{t_2}, \ldots, , \mu_{t_n}\}$ show changes. Each segment represents a process with its own approximately time – invariant mean. In otherwords, the segment boundaries of $\{\mu_{t_1}, \mu_{t_2}, \ldots, , \mu_{t_n}\}$, separate $\{x_1, x_2, \ldots, x_n\}$ into segments with approximately stationary nears within individual segments. The time instants of the segment boundaries,

vii. sorted $\{T_{\mu,1}, T_{\mu,2}, \ldots, T_{\mu,k_\mu}\} \cup \{T_{e,1}, T_{e,2}, \ldots, T_{e,k_e}\}$. We obtain and denote the segments as $\{\bar{x}_1, \bar{x}_2, \ldots, , \bar{x}_{(k_\mu+k_e+1)}\}$, where

$\bar{x}_1 = \{x_1, x_2, ..., X_{T_1}\}$,

$\bar{x}_2 = \{X_{T_{1+1}}, X_{T_{2+2}}, ..., X_{T_2}\}$, … and

$\bar{x}_{(k_\mu+k_e+1)}\}, = \{x_{T_{(k_\mu+k_e)}}+1, x_{T_{(k_\mu+k_e)}}, +2, \ldots, x_n\}$

viii. Compute the means and average entropies of the segments,

$\{\bar{x}_1, \bar{x}_2, ..., \bar{x}_{(K_\mu+K_e+1)}\}$. We denote the pairs of the means and the average entropies, corresponding

to $\{\bar{x}_1, \bar{x}_2, ..., \bar{x}_{(K_\mu+K_e+1)}\}$ by $\{\mu_{\bar{x}_1}, e_{\bar{x}_1}\}$, $\{\mu_{\bar{x}_2}, e_{\bar{x}_2}\} \ldots \{\mu_{\bar{x}_{(K_\mu+K_e+1)}}, e_{\bar{x}_{(K_\mu+K_e+1)}}\}$.

ix. By treating the mean and entropy pairs, $\{\mu_{\bar{x}_1}, e_{\bar{x}_1}\}$, $\{\mu_{\bar{x}_2}, e_{\bar{x}_2}\} \ldots \{\mu_{\bar{x}_{(K_\mu+K_e+1)}}, e_{\bar{x}_{(K_\mu+K_e+1)}}\}$ as points in the R^2, we use the $\{\mu_{\bar{x}_1}, e_{\bar{x}_1}\}$, $\{\mu_{\bar{x}_2}, e_{\bar{x}_2}\} \ldots \mu_{\bar{x}_{(K_\mu+K_e+1)}}, e_{\bar{x}_{(K_\mu+K_e+1)}}\}$, as feature representations of $\{\bar{x}_1, \bar{x}_2, ..., \bar{x}_{(K_\mu+K_e+1)}\}$ in the R^2 plane.

Now we use the K-mean of clustering in [12] on the mean and entropy pairs. The number of clusters can be determined by using the elbow criterion [2] [5], the Davies – Boulding Index [18], or the Dunn Index [9] based on the cluster centers from the K-means clustering. The estimated number of clusters the estimated number of states for the MHSMM, which denotes the number of state transitions, from S_i to S_j in the estimated state sequence $\{\bar{\bar{q}}_1, \bar{\bar{q}}_2, ..., \bar{\bar{q}}_k\}$. This estimation approach for the tpm A is based on the maximum likelihood estimation method [3].

Step 2

The 1 x M steady state probability $\hat{\pi}$can be computed by solving the equation $\hat{\pi} = \hat{\pi}\hat{A}$.

Step 3

The estimated state duration pdfs.

$\{\hat{P}_{dur,s_1}(t), \hat{P}_{dur,s_2}(t), \ldots, \hat{P}_{dur,s_M}(t)\}$, can be computed from $\{\bar{\bar{D}}_1, \bar{\bar{D}}_2, \ldots, \bar{\bar{D}}_k\}$ and $\{\bar{\bar{q}}_1, \bar{\bar{q}}_2, ..., \bar{\bar{q}}_k\}$. For example, those $\{\bar{\bar{D}}_j \mid \bar{\bar{q}}_j = S_i\}$, where $1 \le j \le k$, are treated as realizations of $P_{dur,s_i}(t)$, Thus, the $P_{dur}, S_i(t)$, can be estimated by performing pdf estimation technique on those $\{\bar{\bar{D}}_j \mid \bar{\bar{q}}_j = S_i\}$. The pdf estimation can be performed by using the parametric approaches [1] [7] or non-parametric approaches [18] [13], depending we denote by M. By denoting the clusters is the MHSMM states individually, the states, $\{S_i \mid 1 \le i \le \hat{M}\}$, are created. After K-means clustering, we assign the clusters to their corresponding states in our intended MHSMM, and then assign all the segments to their corresponding states in the MHSMM. In this step, each segment is assigned its own corresponding state in the MHSMM. We denote the estimated states of all the segments as $\{\bar{q}_1, \bar{q}_2, ..., \bar{q}_{(K_\mu+K_e+1)}\}$ which represent the estimated MHSMM states of $\{\bar{x}_1, \bar{x}_2, ..., \bar{x}_{(K_\mu+K_e+1)}\}$ correspondingly.

x. For those segments which are consecutive in the same cluster, we consider them as derived from the our-segmentations of the segmentation algorithm. These consecutive and same-state segments are in fact in the same segment. Hence we combine the consecutive and same-state segments into a single segment. By combing those segments, we form the final estimated segments $\{\bar{\bar{x}}_1, \bar{\bar{x}}_2, ..., \bar{\bar{x}}_k\}$ and the estimated state sequence $\{\bar{\bar{q}}_1, \bar{\bar{q}}_2, ..., \bar{\bar{q}}_k\}$, representing the estimated states of the segments $\{\bar{\bar{x}}_1, \bar{\bar{x}}_2, ..., \bar{\bar{x}}_k\}$ Correspondingly. The durations of the segments are $\{\bar{\bar{x}}_1, \bar{\bar{x}}_2, ..., \bar{\bar{x}}_k\}$ and are denoted by $\{\bar{\bar{D}}_1, \bar{\bar{D}}_2, ..., \bar{\bar{D}}_k\}$. Those estimated segment information, ie. $\{\bar{\bar{x}}_1, \bar{\bar{x}}_2, ..., \bar{\bar{x}}_k\}$, $\{\bar{\bar{q}}_1, \bar{\bar{q}}_2, ..., \bar{\bar{q}}_k\}$, and $\{\bar{\bar{D}}_1, \bar{\bar{D}}_2, ..., \bar{\bar{D}}_k\}$, will be used to perform the state parameter estimation step as given below in 6.4.2. All the segmentation steps are clearly shown in the block diagram in Fig. 2(a).

F. Steps involved in the state parameter estimation

In this step, we use the estimated segment information, i.e. $\{\bar{\bar{x}}_1, \bar{\bar{x}}_2, ..., \bar{\bar{x}}_k\}$, $\{\bar{\bar{q}}_1, \bar{\bar{q}}_2, ..., \bar{\bar{q}}_k\}$, and $\{\bar{\bar{D}}_1, \bar{\bar{D}}_2, ..., \bar{\bar{D}}_k\}$, to estimate the state parameters. Fig 2(b) gives the details of the block diagrams.

Step 1

The elements of the state transition matrix $\hat{A}$can be estimated by $\hat{a}_{ij} = N(S_i \rightarrow S_j) \mid N(S_i)$, for $1 \le i, j \le \hat{M}$, where N $(S_i \rightarrow S_j)$ on whether there are prior knowledge about the family of pdfs.

Step 4

The estimated duration mean, $\hat{\mu}_{dar}(S_i)$, of the state S_i can be computed by the mean of the estimated duration p.d.f in each state, ie,

$\hat{\mu}_{dar}(S_i) = \int t. \hat{P}_{dur} \; S_i(t) \, dt$, for $1 \le i \le \hat{M}$.

Step 5

The estimated acf, $\hat{R}_{s_i}(t)$, of the state S_i can be estimated by computing the time-averaged acfs of the $\{\bar{\bar{x}}_j \mid \bar{\bar{q}}_j = S_i, \; 1 \le j \le k\}$

Step 6

The estimated marginal envelope pdf, $\hat{P}_{s_i}(x)$, in the state S_i can be computed by treating $\{\bar{\bar{x}}_j \mid \bar{\bar{q}}_j = S_i, \; 1 \le j \le k\}$as realizations of $\hat{P}_{s_i}(x)$. The p,d.f estimation method includes the parametric [1] [7] on the non-parametric approaches [18] [13].

Step 7

The steady-state percentage of time in the state S_i can be computed by using (6.1). The estimated overall envelope marginal pdf can be computed by using (6.2).

G. Implementation of the AFSMCM and the HMM for comparisons

(AFSMCM-amplitude-based Finate – state Markov Chain Model)

In order to evaluate the performance of the proposal MHSMM, we compare its performance to those based on alternative approaches of the AFSMCM and the HMM. The methodologies of estimating the parameters of the AFSMCM and the HMM are briefly described here:

The AFSMCM is implemented to have 80 states. In other words, the range of the envelope is divided into 80 intervals. For an AFSMCM with state transition probability a_{ij}, its ML estimate is given by $\hat{a}_{ij} = N(S_i \rightarrow S_j) \mid N(S_i)$ [3], where $N(S_i)$ is the number of S_i and $N(S_i \rightarrow S_j)$ is the number of transitions from S_i to S_j in the observed training sequence.

For the HMM, the range of the envelope is also divided into 80 intervals. The centers of the 80 intervals are the outputs of the states in the HMM. The HMM is implemented to have 4 states. Each state has its own probability mass function (pmf) with the domain spanning over the centers of the 80 envelope intervals. The iterative Baum-welch method with forward-backward variables[16] is implemented to estimate the parameters in the HMM. This approach is optimal in the likelihood sense, although only the local MLE is guaranteed due to the many local maxima in the parameter space [16]. In this study
the parameters of the AFSMCM and the HMM are all estimated using the above mentioned approaches.

H. Simulation

Details given in section 6.2 equations (30) and (31). The ML estimator for Ω in (30) is given by$\widehat{\Omega} = \sum_{i=1}^{n} x_i/n$. For K_R in (30), the moment method gives $K_R = \sqrt{1-\gamma}\,/(1-\sqrt{1-\gamma})$ and

γ = var $[x^2]$ / ((E $[x^2]$)^2). To estimate P_{dur} $S_i(t)$, the parametric approach is used with the log normal distribution. For each state, the parameters of the state duration pdf are estimated individually. The parameters of (31) are estimated by

$\mu_{ln} = ln(E[x] - (\frac{1}{2})\, ln\,(1+ (var[x] / (E[x]^2)))$

and$\sigma^2 = ln\,(1+ (var[x] / (E[x]^2)))$. Those E[x], var [x], and var $[x^2]$ are computed by their time-average counter parts.

In fig.2, the elbow criterion, the Davis-Bouldin Index, and the Dunn Index consistently indicate 4 as the suggested number of cluster centers. Thus, the 4-state MHSMM was used to model this fading sequence. By performing the proposed parameter estimation scheme, the results are shown in fig.2a and fig.2b. In fig.2a, the theoretical p.d.f is computed by the parameters specified in simulation. The estimated MHSMM p.d.f and the AFSMCM p.d.f are close to the theoretical p.d.f.

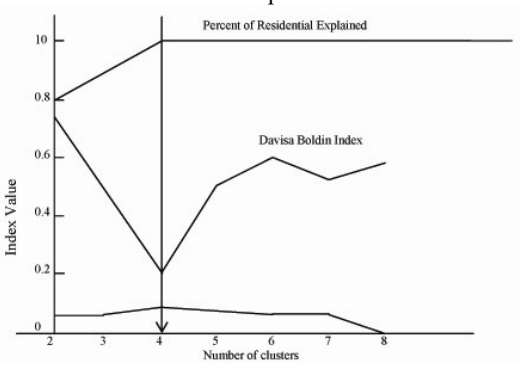

Fig.2 The elbow criterion, the minimum of the Davis-Bouldinindex,and the maximum of the Dunn index indicate 4 as the number of clusters

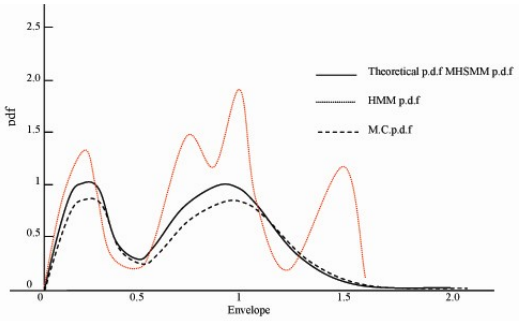

Fig.2.a The theoretical pdf, the estimated HSMM pdf, the estimated AFSMCM pdf, and the estimated HMM pdf.

The HMM pdf can be seen to obviousy deviate from the theoretical pdf. We also compare the estimated cdfs with the theoretical cdf by the KS-test. The D-statistics, from the KS-test, of the MHSMM cdf, the AFSMCM cdf, and HMM cdf are 0.0218, 0.0638 and 0.1692, which shows that the MHSMM has the best-fitted pdf among the 3 models.

The estimated acf of the 4 states in the MHSMM are shown in fig.3 below. For comparisons, the theoretical Clarke acf are also shown in fig.3. The acts of the MHSMM are shown closely characterize the theoretical acfs in different situations.

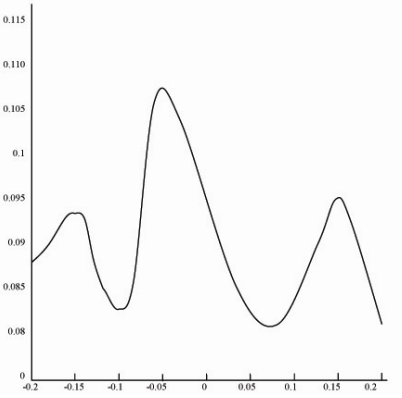

Fig.2.b

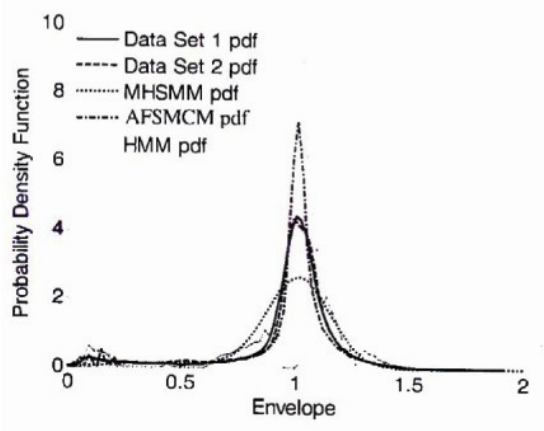

Fig.3

I. Experiments

Experiments we conducted in two types of areas

i. One is a Hill area and the measurements are from a two storied building.
ii. A village area with natural scenario with trees of all type. Here also data were collected from the top of a two storied building.

In both the experiments, the carrier frequency was set as 2.4 GHZ. The signal envelope was collected at 200 samples per second. The measurements of 4000 seconds were collected, individually from each experiment. The data for 4000 seconds, from each scenario, were separated into the first 2,000 seconds, denoted as the data set 1, and the second 2000 seconds denoted as the data set 2. Our objective here is to use the data set 1 to estimate the model parameters, and then use the data set 2 to test the accuracies.

Experiment 1 area is semi-open due to hills on one side, with reflectors and scatters surrounding the transmitter and receiver. The dynamics of the fading channel were caused by a pre-arranged personnel walking through the LOS path of the channel. The candidate walked back and forth periodically at a regular walking speed. The experiment was conducted at the time when the place (site) was quiescent without other non-cooporating dynamic fading disturbances, with the pre-arranged person being the only dynamic channel disturbance.

The number of clusters is suggested to be two by the elbow criterion, Davis-Boudin Index, and the Dunn Index. Thus, the two-state MHSMM is employed to further estimate the state parameters. The data pdfs in Fig.4 are constructed by the Kernal Density Estimation (KDE) method [21] [22]. The estimated MHSMM pdf is very close to the data pdfs for both the data sets 1 and 2, as shown in Fig.4. Comparing the empirical cdf of the data set 1 with the estimated cdfs of the models, the D-statistics from the KS-test are 0.2166 (MHSMM), 0.0772 (AFSMCM), and 0.3114(HMM), which show that the AFSMCM has the best-fitted pdf. Comparing empirical cdf of the data set 2 with the model cdfs estimated by the data set 1, the D-statistics of the KS-test are 0.1636 (MHSMM), 0.1395 (AFSMCM), and 0.2443 (HMM), which show that the AFSMCM also has the best-fitted pdf. The estimated acfs of the MHSMM and the acfs of the corresponding theoretical Clarke model are shown in fig.6, where the MHSMM acfs closely characterize the theoretical acfs. Although, in this case, the AFSMCM is slightly better in fitting the pdfs, it is found that the capability of fitting the pdf is only one of the performance metrics for fading models. For characterizing the acfs, the MHSMM shows more flexibility. Thus, while selecting models, the model accuracies and also the flexibilities need to be considered based on specific applications.

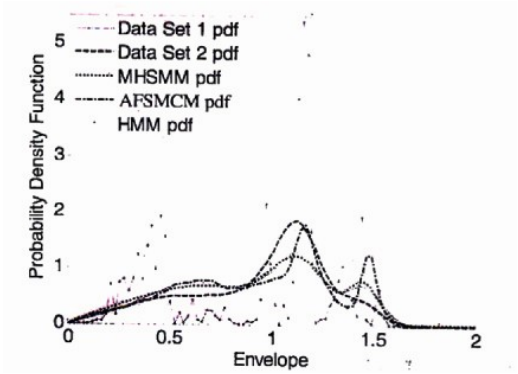

Fig.4

Experiment, as said, was conducted in the village on the top of a building. The transmitter and the receiver were in the NLOS positions. The experiment was conducted in the morning when the area is busy. The dynamics of the fading channel were caused by many non-cooperating persons, walking through or waiting. We did not intend to put any controlled dynamic fading disturbances. This step was intended to capture the fading channel characteristics under normal busy hall way conditions.

The number of clusters is suggested to be four by the already mentioned criteria. Thus, the four state MHSMM is employed to further estimate the state parameters. The estimated pdf of the MHSMM is close to the data pdfs, constructed by the KDE method, from both the sets 1 and 2, as shown in Fig.5 comparing the empirical cdf of the data set 1 with the estimated model cdfs, the D-statistics of the KS test are 0.0275 (MHSMM), 0.0434(AFSMCM), and (0.1644) (HMM), which implies that MHSMM is the best-fitted. Comparing the empirical cdf of the data set 2 with the model cdfs estimated by the data set 1, the D-statistics of the KS-test are 0.0698 (MHSMM), 0.0735 (AFSMCM), and 0.1522 (HMM), which again shows the superiority of MHSMM as the best-fitted. The estimated acfs of the MHSMM and the acfs of the corresponding theoretical Clarke model shown in

Fig.7, where the MHSMM acfs closely characterize the theoretical acfs. Summarizing the results from both experiments in station I and II, we can conclude the superiority of the MHSMM as comparable to that of the AFSMCM in characterizing the acfs.

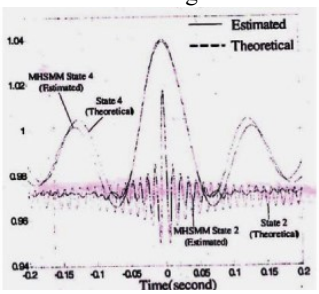

Fig. 5

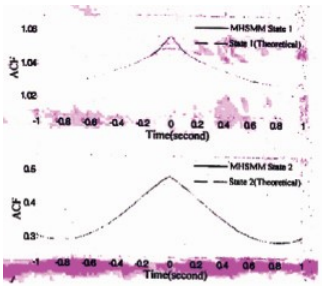

Fig.6

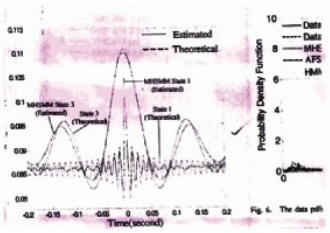

Fig.7

J. Inferences

In the HMM and the Hidden Semi-Markov Model (HSMM), there exist iterative algorithms which adjust the model parameters to increase the likelihood [16], based on the iterative Bawn-Welch algorithm with the forward-backward variables. However the iterativealgorithms remain to be improved in the following aspects. First, we need to know the number of states, outputs of the states etc., in order to apply the iterative algorithm. In the real applications, we lack the required information about the number of states and outputs of the states, which can only by chosen heuristically. Apart from this, the iterative algorithms often achieve local maxima. The MLE is difficult to achieve in practice. Secondly, the formulation of the iterative algorithm is mathematically tractable under the assumption on the process ie the outputs at different time instants are un-correlated. In the colored non-gaussian process, the iterative algorithms are difficult to formulate explicitly. In contrast to these limitations, the MHSMM is designed to the freedom in characterizing the acfs.

While estimating the pdfs of $P_{dur,s_i}(t)$,, and $P_{s_i}(x)$, we can use parametric or non-parametric approaches. If priori` knowledge about our interested scenario is available, we may consider using the prior-known family of pdfs, the pdf estimation problem is reduced to estimate the parameters of the family of pds. If there is no priori information available the non-parametric approaches must be employed, e.g. the kernel density estimation approach [13], [18]. In our proposed MHSMM parameter estimation scheme, the length of the window is an important factor which influences the results. We here use to following situations in determining the length of the window: (i) The accuracy requirements of the state transition times, related to the applications, are considered. For example, the power control interval of the GSM system is specified to be 480 ms[8]. When the fading model is employed to facilitate the power control, the un-certainties of the estimated state transition times is required to be not much larger than the power control interval. The windows much larger than the power control interval cause large uncertainties in the estimated state transition times and lead to adverse effects in the power control. (ii) The length of the window must be much smaller than the average state durations, such that the temporal uncertainty caused by the window length is negligible. For the examples in the 4 states, the LOS, the NLOS, the high speed, and the low speed conditions are expected to persist longer than tens of seconds. Thus, the length of the window most be much smaller than these durations (iii) The parameter estimation scheme uses the entropy of the energy distribution in the frequency domain. To accurately calculate the entropy, the principle of uncertainty and the U-shaped power spectral density of clark model must be considered. Based on the principle of uncertainty, the $\Delta f \Delta t \geq ¼ \pi$, where Δf is the bandwidth of the signal and Δt is the window length of the signal. In the clark model, the U-shape power spectral density of the channel process is non-negligible from-f_D to f_D. Hence we obtain $\Delta f = 2f_D$ and then $\Delta t \geq 1/(4 \pi \Delta f) = 1/(8 \pi f_D)$.

For accurately estimating the MHSMM parameters, we need to obtain sufficient data. In mobile scenerios, the state statistics, which are dominated by the physical processes, e.g. the LOS, the NLOS, the high speed, and the low speed scenarios, often persist at sufficient temporal durations for data collections to characterize these physical conditions.

The experimental results show the feasibility of collecting sufficient data for the parameter estimation.

VII. Conclusion

In this study, the use of MHSMM for characterizing the flat fading envelope process. The study also provide associated parameter estimation algorithms in this model. The use of the MHSMM is to match various physical fading conditions into the process of the states of the MHSMM. Thus, the MHSMM is capable of modeling the piece-wise

stationary properties of the envelope process, including the envelope pdfs and the acfs. In the parameter estimation scheme, the observed envelope sequence is segmented and the segments are used to estimate the model parameters. The parameters of the state envelope pdfs, the acfs, and the state duration pdfs can be estimated by using either non-parametric approaches or parametric approaches, depending on the availability of the prior knowledge. We demonstrated an example on the GSM system parameters under different physical fading conditions including mobility speeds and shadowing. These results showed acceptable accuracies for the MHSMM and the associated parameter estimation scheme. The parameters of the AFSMCM and the HMM were also estimated based on the simulation data. Comparison of the estimated results of the three methods, it shows that MHSSM is able to provide the most feasible and accurate results in modeling this simulation scenario. Apart from simulations, the experimental data from the two sites were collected and separated into two non-overlapping sets. One set of the data was used to estimate the model parameters, while the other set is used to compare and verify their accuracies. These experimental data also verified the accuracies and theflexibilities of the MHSMM and the associated parameter estimation scheme.

REFERENCES

[1] A.Abdi, C.Tepedelenlioglu, M.Kaveh and G.Ginnakis (2001), "On the estimation of the K parameter for the Rice fading distribution", IEE commun. Lett. 5, 92-94.

[2] M.S.Aldenderfer and R.K. Blashfield (1984, "Cluster Analysis", Newbury Park, CA:Sage Press.

[3] T.W.Anderson and L.A. Goodman (1957), "Statistical inference about Markov Chains"; Annals Mathematical statistics, 28, 89-110.

[4] L.E.Baum, T.Petrie, G.Soules an N.Weiss (1970), "A maximization technique occurring in the statistical analysis of probabilistic functions of Markov Chains", Ann. Math. Stat, 41,164-171.

[5] J.C.Bezdek and N.R.Pal, 'Some new indexes of cluster validity", IEEE Trans. Systems, Man Cybernetics, Part B.Val.28, No.3; 301-315.

[6] R.H.Clarke (1968); "A statistical theory of mobile radio reception", Bell. Syst.Tech. J.47, 957-1000.

[7] E.I.Crow and K.Shinmizu (1988), Lognormal Distributions: Theory and Applications, N.Y. Marcel Dekker.

[8] Digital Cellular telecommunication system (phase 2+); "Radio transmission and reception", ETSI TS100 910 v8.26.0 (2005-11) (online) available at: http||www||.elsi.org|

[9] D.L.Devices and D.W.Bouldin (1979); "A cluster separation measure" IEEE Trans.Pattern Analysis and Machine Intelligence, 1, 274-227.

[10] J.C.Dunn (1973); "A fuzzy relative of the ISODATA process and its use in detecting compact well-separated clusters"; J.Cybernetics, 3, 32-57.

[11] E.N.Gillbert, (1960), "Capacity of a burst-noise channel", Ball syst Tech. T.39, 1253-1265.

[12] A.K.Jain and R.C.Dubes (1988); "Algorithms for clustering Data. Upper Saddle River", NJ. Prentice-Hall; Inc.

[13] M.C.Jones, J.S.Marron and S.J.Sheathen (1996); "A brief survey of bandwidth selection for density estimation"; J.American statistical Association, 91, 401-407.

[14] E.Keogh, S.Chu, D.Hart and M.Pozzani (2003), "Segmenting time series: a survey and novel approach", Data mining in Time series data bases. World scientific pub.company.

[15] J.G.Proakis, (1986), "Digital Communications, New York : the Graw-Hill"

[16] R.Rabinaer (1969), "A tutorial on hidden Markov Models and selected application in speech recognition", Proc. IEEE 77, 257-286.

[17] M.Sayadieh, F.R.K.Schischang and A.Len-Garcia (1996), "A block memory model for correlated Rayleigh fading channels", in Proc IEEE Intconfcommun. Dallas, TX, 282-286.

[18] S.Silverman and B.W.Silverman (1986); "Density Estimation for Statistics and Data Analysis" CRC Press.

[19] W.Turon (1998), "Performance Analysis of Digital Transmission systems", 2nd ed. N.Y.Computer Science.

[20] W.Turin and M.M.Sondhi (1993), "Modeling error sources in digital channels", IEEE, J.Select, Areas commn. 11, 340-347.

[21] W.Turin (1998); "Digital Transmission systems: performance Analysis and Modeling", N.Y: Mc.Graw-Holl.

[22] H.S.Wang and N.Moayeri, (1995), "Finate-State Markov Channel-A useful model for radio communication Channels"; IEEE Trans. Veh. Technol, 44, 163-171.